Article

On the Thermal Stability of Selected Electrode Materials and Electrolytes for Na-Ion Batteries

Ruslan R. Samigullin [ID], Zoya V. Bobyleva [ID], Maxim V. Zakharkin, Emiliya V. Zharikova, Marina G. Rozova, Oleg A. Drozhzhin *[ID] and Evgeny V. Antipov [ID]

Department of Chemistry, Lomonosov Moscow State University, Leninskie Gory 1-3, Moscow 119991, Russia; ruslan.samigullin.rinatovich@yandex.ru (R.R.S.); evgeny.antipov@gmail.com (E.V.A.)

* Correspondence: drozhzhin@elch.chem.msu.ru

Abstract: Sodium-ion batteries are a technology rapidly approaching widespread adoption, so studying the thermal stability and safety of their components is a pressing issue. In this work, we employed differential scanning calorimetry (DSC) and ex situ powder X-ray diffraction to study the thermal stability of several types of sodium-ion electrolytes ($NaClO_4$ and $NaPF_6$ solutions in PC, EC, DEC, and their mixtures) and various cathode and anode materials ($Na_3V_2(PO_4)_3$, $Na_3(VO)_2(PO_4)_2F$, β-$NaVP_2O_7$, and hard carbon) in combination with electrolytes. The obtained results indicate, first, the satisfactory thermal stability of liquid Na-ion electrolytes, which start to decompose only at 270~300 °C. Second, we observed that charged vanadium-based polyanionic cathodes, which appear to be very stable in the "dry" state, demonstrate an increase in decomposition enthalpy and a shift of the DSC peaks to lower temperatures when in contact with 1 M $NaPF_6$ in the EC:DEC solution. However, the greatest thermal effect from the "electrode–electrolyte" interaction is demonstrated by the anode material: the heat of decomposition of the soaked electrode in the charged state is almost 40% higher than the sum of the decomposition enthalpies of the electrolyte and dry electrode separately.

Keywords: Na-ion batteries; differential scanning calorimetry; thermal stability; electrode material; electrolyte; cathode; anode

1. Introduction

Lithium-ion batteries (LIBs) are the most efficient electricity storage solution available today, and their applications have steadily expanded over the past thirty years. Yet, the safety of LIBs is an extremely important issue, which has become the subject of many studies during the last decades [1–13]. It mainly concerns the thermal stability of the charged electrode materials, electrolytes, and their combinations. In general, the accumulated experimental experience consists of the following theses: (a) oxide cathode materials are less stable than phosphate ones, although the release of oxygen when heating charged cathodes occurs in both cases; (b) in combination with an electrolyte, decomposition processes, as a rule, occur more intensely and at lower temperatures; (c) anode materials (primarily graphite) demonstrate enthalpies of decomposition that are several times higher than cathode ones. Sodium-ion batteries (SIBs), which are considered the most likely successors to LIBs in many areas of technology, may also cause certain operational safety issues, and, in recent years, there has been active research devoted to the thermal stability of their components [14–23]. Thus, the analysis of the thermal behavior of Prussian blue analogs revealed the generation of toxic cyanides and their exothermic reactions with electrolytes, indicating that PBA cathodes may bring safety concerns to nonaqueous Na-ion batteries [18,19]. Zhang et al. studied the thermal stability of hard carbon in the presence of an electrolyte at different states of charge and showed that the thermal effect of decomposition varies from 1.9 kJ/g for an initial electrode (2.5 V vs. Na/Na$^+$) to 3.0 kJ/g

for an electrode at a potential of 0 V vs. Na/Na$^+$, which is close to the values for a metallic sodium anode (3.6 kJ/g). [20]. Mohsin et al. demonstrated an increase in enthalpy and a decrease in the temperature of decomposition peaks for the Na$_3$V$_2$(PO$_4$)$_3$ cathode and hard carbon anode materials with increasing their degree of charge [21]. Samigullin et al. conducted a systematic study of the thermal stability of several charged materials for LIBs and SIBs in the absence of an electrolyte, demonstrating the advantages of polyanionic vanadium compounds over oxides and carbon materials [22,23]. A natural question arises regarding the stability of such systems in the presence of an electrolyte, as well as the stability of the liquid electrolytes themselves. A significant difference in the thermal stability of LIB electrode materials between dry and electrolyte-soaked states, due to certain chemical interactions, was previously observed [3,6,24]. It was shown that polyanionic cathodes, such as LiFePO$_4$ (LFP) or LiFe$_{1-x}$Mn$_x$PO$_4$ (LFMP), that begin to decompose at 300–400 °C in the absence of an electrolyte, demonstrate a strong decrease in the onset temperature of the exothermic process, i.e., down to 200–250 °C [3,24,25]. Most authors consider PF$_5$, produced from the decomposition of LiPF$_6$ during the initial stage of heating, to be the most reactive component of the reaction media. On the other hand, NaPF$_6$ salt has a better thermal stability with a higher decomposition temperature [11,26,27]. Therefore, the behavior of the "electrode-electrolyte" composition in the Na-ion system seems quite ambiguous and worth studying. In the recent paper, Gan et al. conducted a systematic study of the thermal stability of the NaNi$_{1/3}$Fe$_{1/3}$Mn$_{1/3}$O$_2$ (NaNFM) cathode material in different Na-ion electrolytes and revealed its better compatibility with NaPF$_6$- and NaTFSI-based solutions; the combination of ethylene carbonate and diethyl carbonate demonstrated better thermal behavior then propylene-carbonate-based electrolytes [28].

In this work, we investigated the thermal stability of several types of electrolytes (NaClO$_4$ and NaPF$_6$ solutions in propylene carbonate (PC), ethylene carbonate (EC), diethyl carbonate (DEC), and their mixtures), as well as cathode and anode materials (Na$_3$V$_2$(PO$_4$)$_3$ (NVP), Na$_3$(VO)$_2$(PO$_4$)$_2$F (NVOPF), β-NaVP$_2$O$_7$ (NVPO), and hard carbon) in combination with electrolytes utilizing differential scanning calorimetry (DSC) and ex-situ powder X-ray diffraction (PXRD).

2. Materials and Methods

2.1. Material Preparation

All electrode materials were synthesized according to previously published routes. All the initial reagents were purchased from Merck (formerly Sigma Aldrich, Rahway, NJ, USA). Briefly, the synthesis procedure is as follows.

2.1.1. Na$_3$V$_2$(PO$_4$)$_3$ (NVP)

The Na$_3$V$_2$(PO$_4$)$_3$ sample was prepared by a two-step synthesis. In the first step, vanadium oxide and citric acid were dissolved in distilled water in a molar ratio of 1:3, followed by stirring for 40 min at 70 °C. Then, a solution of sodium dihydrogen phosphate in distilled water was added dropwise and stirred for another 40 min, after which the solution was evaporated overnight at 95 °C. The solid residue was ground in a mortar and annealed at 350 °C for 3 h under argon, after which it was ground in a SPEX-8000M vibration mill for 5 min and annealed at 750 °C for 8 h under argon [29].

2.1.2. Na$_3$(VO)$_2$(PO$_4$)$_2$F (NVOPF)

V$_2$O$_5$, NaF, NH$_4$H$_2$PO$_4$, and oxalic acid were mixed in 1:3:2:2 molar ratio. Then, the initial precursors were dissolved in deionized water, and the solution was magnetically stirred at 65–70 °C for about 30 min while adding 1 mL of ammonia solution (25 mass%). Next, 5 mL of the obtained homogeneous solution was transferred to a 10 mL glass vessel, placed into a microwave hydrothermal reactor Anton Paar 400 and treated at 180 °C for 30 min. The final solid products were centrifuged and washed with deionized water several times and dried in air. To obtain carbon coating, the material was mixed with glucose

(8 wt.%) in a mortar to receive homogeneous mixture. Then, the mixture was annealed at 600 °C for 1 h under Ar flow [30].

2.1.3. β-NaVP$_2$O$_7$ (NVPO)

The sample was synthesized in two stages. At the first stage, the synthesis was carried out using the hydrothermal method. At the second stage, the obtained precipitate was annealed in an inert atmosphere. The hydrothermal stage was carried out according to the following scheme. The initial reagents—VOSO$_4$, NaOH, H$_3$PO$_4$, and N$_2$H$_6$SO$_4$—were dissolved in distilled water at room temperature with constant stirring. Then, the solution was poured into a Teflon beaker, loaded into a steel autoclave (50 mL). The autoclave was heated with stirring and maintained at 230 °C for 24 h. After that, the autoclave was cooled in air or subjected to rapid cooling under a stream of cold water. The resulting powder was centrifuged (3000 rpm, 3 min) with repeated washing with distilled water and dried in air. At the second stage, the obtained samples were annealed in a furnace at 650 °C in an argon flow (gas flow rate of 10 mL/min, heating time of 3 h) with preliminary argon purging for 30 min [31].

2.1.4. Hard Carbon (HC)

First, D-glucose powder was caramelized in air at 200 °C for 24 h. Then, obtained precursor was powdered in an agate mortar. The second step of the synthesis was annealing at 1300 °C under argon flow for 1 h. The obtained HC material was ground at 400 rpm in a ball mill (Fritsch Pulverisette 5 classic line) for 1 h [32].

2.1.5. Electrodes

For the preparation of the electrodes, all powders were mixed with super P carbon black (Timcal, Willebroek, Belgium) and polyvinylidene fluoride (PVdF, Kureha Chemical, Tokyo, Japan) in a weight ratio of 80:10:10 with N-methyl-2-pyrrolidone (NMP) as the solvent. The homogenous slurry was cast on an aluminum foil by the Doctor Blade technique. The cast sheet was dried at 80 °C to remove NMP, roll-pressed, and punched into 10 or 16 mm diameter electrodes. Subsequently, the punched electrodes were dried at 120 °C under vacuum, and then taken for cell assembly.

2.2. Characterization

The electrochemical measurements were carried out using two-electrode half-cells with hard carbon, NVP, NVOPF, and NVPO as the working electrode; sodium metal as the counter electrode; and glass fiber (Schleicher & Schuell MicroScience, Dassel, Germany) as the separator. Electrolytes were prepared by dissolving NaPF$_6$ or NaClO$_4$ in the corresponding solvents: PC, EC, and DEC, pre-dried with molecular sieves. All electrolyte components were supplied by Merck (formerly Sigma Aldrich, Rahway, NJ, USA) and Kishida Chemicals. Electrochemical cells were assembled in an Ar-filled glove box (MBraun, Garching, Germany). Galvanostatic experiments were carried out using an Elins P-20X8 potentiostat-galvanostat (ES8 software, v. 4.192).

Thermal stability of the electrode materials was investigated by differential scanning calorimetry (DSC) using a Netzsch DSC 204 F1 Phoenix instrument (Selb, Germany) within the temperature range 50–450 °C (5 °C·min^{-1} heating rate) in an argon atmosphere. Electrodes from fully charged "half-cells" were extracted, washed with DMC, and dried under vacuum, and then electrode materials were scrapped from the current collector. The resulting powders (about 6 mg), either separately or in the presence of an electrolyte (about 5 μL), were placed in sealed crucibles made of high-pressure Cr–Ni stainless steel in an Ar-filled glove box. The electrode powder/electrolyte mass ratio was 1:1 to ensure an excess of the electrolyte during the experiment. To calculate the magnitude of the thermal effect, the area under the peak on the DSC curve was considered with subtraction of the background (if any) using the Netzsch Proteus 6.0 software.

Morphology of the samples was investigated using a JEOL JSM-6490LV (Tokyo, Japan) scanning electron microscope (SEM). The phase composition of the electrodes (ex situ experiments) was investigated by powder X-ray diffraction (PXRD) data assembled from a Huber Guinier camera G670 (Image Plate detector, curved Ge (111) monochromator, and CuKα_1 radiation λ = 1.54051 Å) (Rimsting, Germany).

3. Results

First, we performed the DSC experiments in several types of liquid Na-ion electrolytes often used in research works (Figure 1). PC, EC, and DEC were chosen as co-solvents.
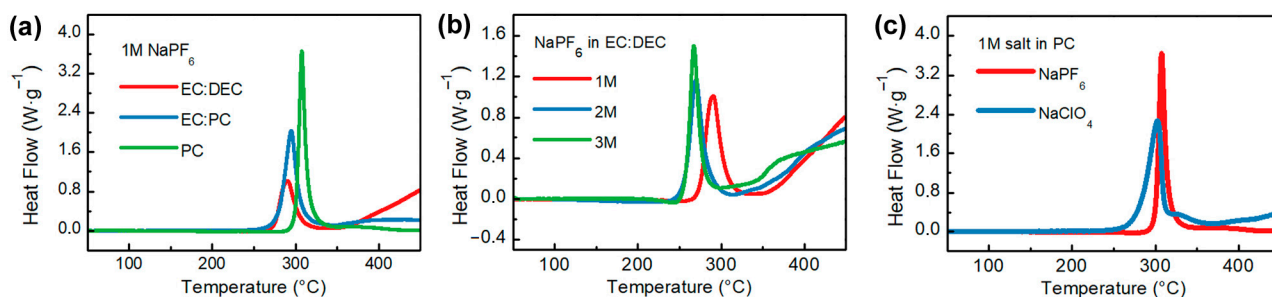
Figure 1. DSC curves for different electrolyte solutions: (**a**) 1M NaPF$_6$ in EC:DEC, EC:PC, and PC; (**b**) 1M, 2M, and 3M NaPF$_6$ in EC:DEC; and (**c**) 1M NaPF$_6$ and NaClO$_4$ in PC.

The results of the studies on 1M NaPF$_6$ solutions in various solvents do not clearly indicate a definitive advantage for any particular type of electrolyte. Although a PC-based electrolyte has a higher temperature of the onset and peak of decomposition (Table 1), the heat released is 1.7 times greater than in the case of 1M NaPF$_6$ in the EC:DEC solution. Similar results were published earlier when comparing solutions of sodium salts in PC and a mixture of EC and dimethyl carbonate (DMC) [10].

**Table 1.** DSC data for different electrolyte solutions.

Electrolyte	Onset Temperature, °C	Peak Temperature, °C	Enthalpy, J·g^{-1}
1M NaPF$_6$ in EC:DEC	274	290	268
2M NaPF$_6$ in EC:DEC	258	270	281
3M NaPF$_6$ in EC:DEC	257	267	246
1M NaPF$_6$ in PC	301	307	476
1M NaPF$_6$ in PC:EC	279	295	456
1M NaClO$_4$ in PC	279	302	629

The study of electrolytes with various NaPF$_6$ concentrations indicates that the thermal stability decreases with an increasing amount of salt in the solution. This observation may seem to contradict the common point of view regarding the better safety of concentrated electrolytes in a lithium-ion system. However, early works devoted to the unique properties of concentrated solutions were concerned rather with the lower volatility of the organic solvent in such systems, whereas later studies using DSC and accelerated rate calorimetry (ARC) revealed a decrease in the decomposition onset temperature with the increasing concentration of lithium salts in different solvents [33–35]. Hence, our data for the concentrated sodium electrolytes are in good agreement with the results previously published for lithium-ion systems, as well as with our experiments. As for the salts, according to our data, the decomposition enthalpy in the case of the NaClO$_4$-based solution is approx. 1.5 times higher than for the NaPF$_6$ solution (Figure 1c, Table 1).

In general, the better stability of sodium-ion electrolytes compared to lithium-ion ones is worth noting. Research shows that solutions of LiPF$_6$ in alkyl carbonates have an S–type decomposition curve, with an endothermic peak of LiPF$_6$ decomposition followed by an exothermic reaction of the interaction between PF$_5$ (a strong Lewis acid) and solvent

components [3,6,7]. The position of the decomposition peak of 1M LiPF$_6$ solutions varies slightly among different studies but is generally within the range of 230–260 °C. In contrast, the Na-ion electrolyte demonstrates a higher temperature of the exothermic peak without any signs of endothermic salt decomposition (this effect is slightly noticeable only in a 3M NaPF$_6$ solution; Figure 1b), which suggests a safety advantage of SIBs.

The obtained electrode materials (their morphology is shown in Figure 2a) demonstrated typical electrochemical properties, with discharge capacities (Figure 2b) in the range of 83–95% of the theoretical ones. Detailed information about the crystal structure, phase composition, and electrochemical properties of the studied electrode materials is provided in previous publications [29–32].
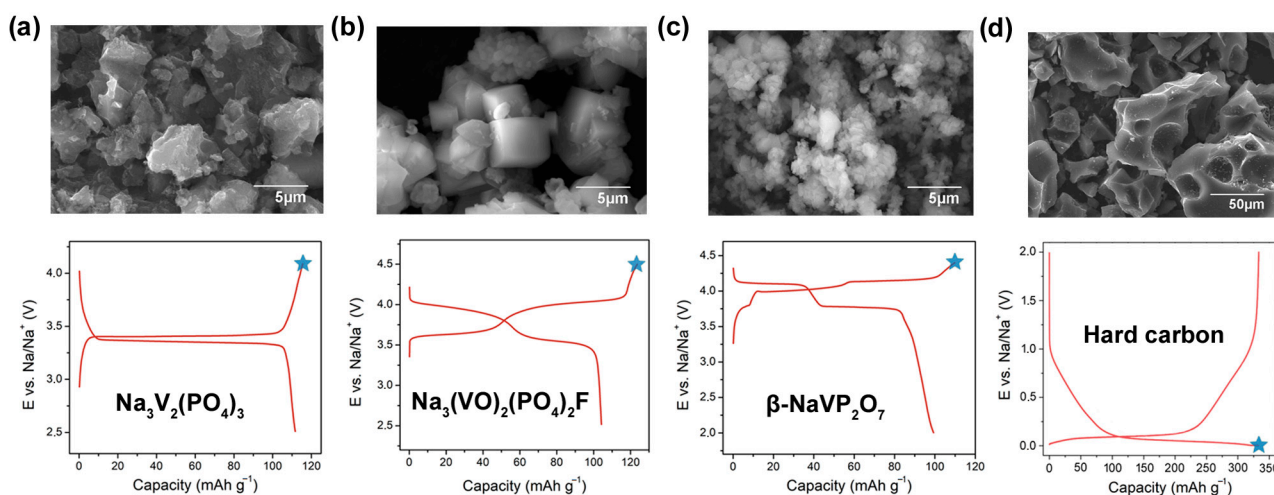

Figure 2. SEM images and charge–discharge curves for the electrode samples: Na$_3$V$_2$(PO$_4$)$_3$ (**a**), Na$_3$(VO)$_2$(PO$_4$)$_2$F (**b**), β–NaVP$_2$O$_7$ (**c**), and hard carbon (**d**). Points on the curve where the electrodes were tested are marked with an asterisk.

The study of Na-ion cathode materials reveals the following pattern. Desodiated vanadium-based polyanionic cathodes—Na$_3$V$_2$(PO$_4$)$_3$, Na$_3$(VO)$_2$(PO$_4$)$_2$F, and β–NaVP$_2$O$_7$—demonstrate a significant increase in the decomposition enthalpy in the presence of an electrolyte compared to their "dry" state (Figures 3a–c and 4). Here and below, the thermal effect of the mixture is normalized to the mass of the electrode material. In the absence of chemical interaction, this effect is defined as:

$$\Delta H_{electrode+electrolyte} = \Delta H_{electrode} + \Delta H_{electrolyte}.$$

Moreover, the decomposition onset temperature of vanadium-based polyanionic cathodes soaked in electrolytes is greatly reduced compared to their dried state, and even lower than that of the liquid electrolyte. This can be a consequence of the increased reactivity of vanadium in high oxidation states with the electrolyte components. This effect was observed by S. Whittingham's group in delithiated LiVOPO$_4$. The authors suggested that the interaction between the charged material (VOPO$_4$) and the solvent in the electrolyte is accelerated by LiPF$_6$, and they proposed 11 possible chemical reactions to describe this process [3]. In the present work, we have obtained similar results for all three studied vanadium-containing cathode materials in the presence of an electrolyte, i.e., a strong decrease in the onset temperature of exothermic processes compared to "dry" materials and electrolytes. Notably, in the case of charged Na$_3$(VO)$_2$(PO$_4$)$_2$F and β–NaVP$_2$O$_7$ (Na(VO)$_2$(PO$_4$)$_2$F and β–VP$_2$O$_7$, correspondingly), the first decomposition peak appears at 170~180 °C. However, this temperature is higher for Na$_1$V$_2$(PO$_4$)$_3$, reaching ~225 °C (Figure 4).
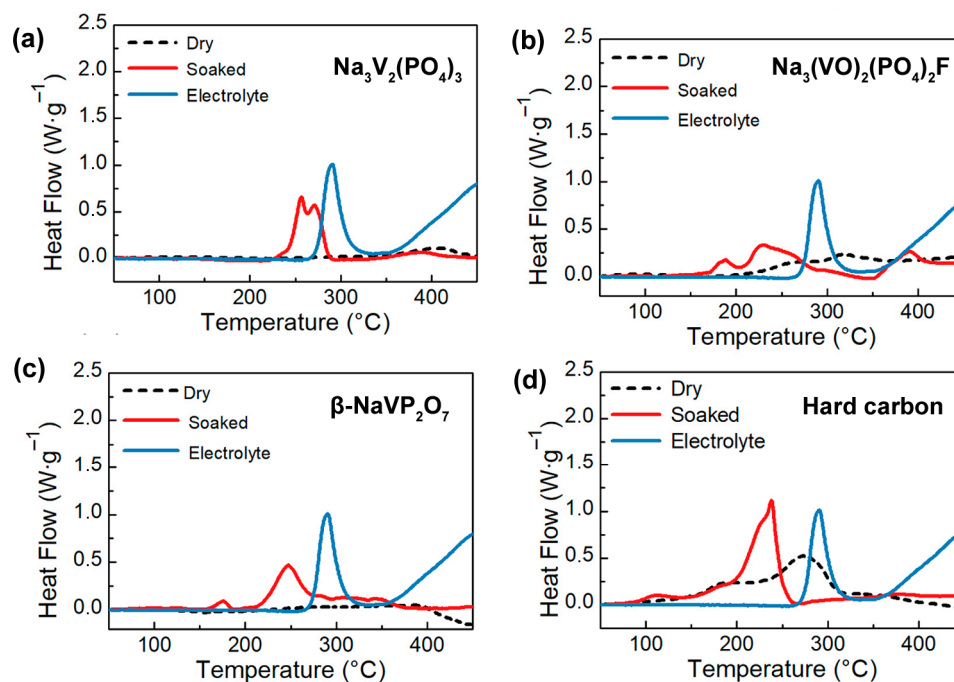
Figure 3. DSC curves (red line) for the charged electrode materials soaked in electrolyte: $Na_3V_2(PO_4)_3$ (**a**), $Na_3(VO)_2(PO_4)_2F$ (**b**), β–$NaVP_2O_7$ (**c**), and hard carbon (**d**). For comparison, DSC curves for the dried electrodes (dot line) and 1M $NaPF_6$ in EC:DEC electrolyte (blue line) are also plotted.
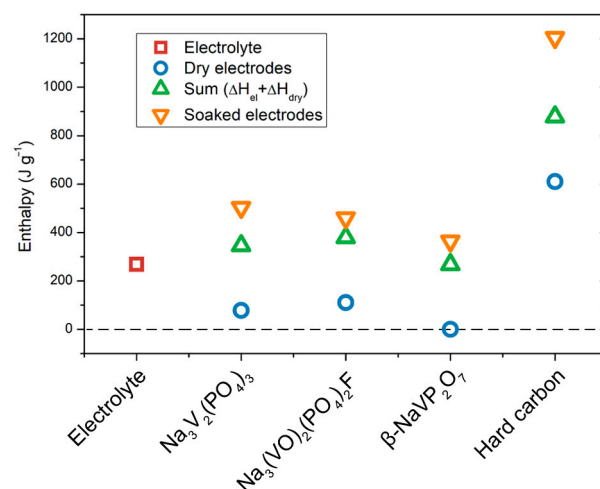
Figure 4. Schematic representation of the data on the enthalpy of dried [20] and soaked electrodes.

Recently, Pablos et al. studied the thermal stability of $Na_{3-x}V_2(PO_4)_2F_3$ and $Na_{3-x}V_2(PO_4)_2F_{3-y}O_y$ at different states of charge and observed a similar low-temperature decomposition peak at a high desodiation state in all samples (x = 2) [36]. According to our findings and literature data, the onset of interaction between the charged vanadium-containing material and the electrolyte during heating is largely determined by the degree of oxidation of vanadium cations, i.e., the desodiation potential. Additionally, an increase in the charging potential leads to a change in the quantity and composition of electrolyte oxidation products at the cathode–electrolyte interface, potentially decreasing the temperature at which the material starts to decompose. Thus, in the work of Samigullin and co-authors, an increase in the enthalpy and a decrease in the onset temperature of the decomposition process for $Na_3V_2(PO_4)_3$ charged at a higher potential (4.5 versus 3.8 V vs. Na/Na^+) were found [22]. Considering that, at 3.8 V, the material is already completely charged, it was

concluded that the decrease in thermal stability was associated precisely with an increase in the amount and reactivity of the CEI (cathode–electrolyte interface) components.

In terms of decomposition enthalpy, β–NaVP$_2$O$_7$ remains the most stable among the studied cathode materials despite exhibiting the highest charging potential and the lowest onset temperature (Table 2). This is likely due to the well-known stability of the pyrophosphate group, as well as the fact that the main product of the electrode–electrolyte reaction, α–NaVP$_2$O$_7$, is quite similar to β–VP$_2$O$_7$ in terms of its composition and structure (Figure 5) [31].

Table 2. DSC data and phase composition of the charged electrodes after the DSC experiment in the presence of electrolyte (ex situ PXRD).

Initial Sample	Onset Temperature, °C	Peak Temperature, °C	Enthalpy, Dry *, J·g^{-1}	Enthalpy, Soaked, J·g^{-1}	Main Crystalline Phases by Ex Situ PXRD
Na$_3$V$_2$(PO$_4$)$_3$	243	256, 270	78	503	α–NaVP$_2$O$_7$
Na$_3$(VO)$_2$(PO$_4$)$_2$F	170	188, 229, 391	111	460	Na$_5$V$_3$O$_3$F$_{11}$
β–NaVP$_2$O$_7$	150	175, 247	–	364	α–NaVP$_2$O$_7$
Hard carbon	85	114, 238	610	1205	NaF
Electrolyte (1M NaPF$_6$ in EC:DEC)	274	290		268	

* Data for the charged, washed, and dried electrode materials obtained in our previous study [23]. All calculations are normalized to the weight of the "dry" electrode material.
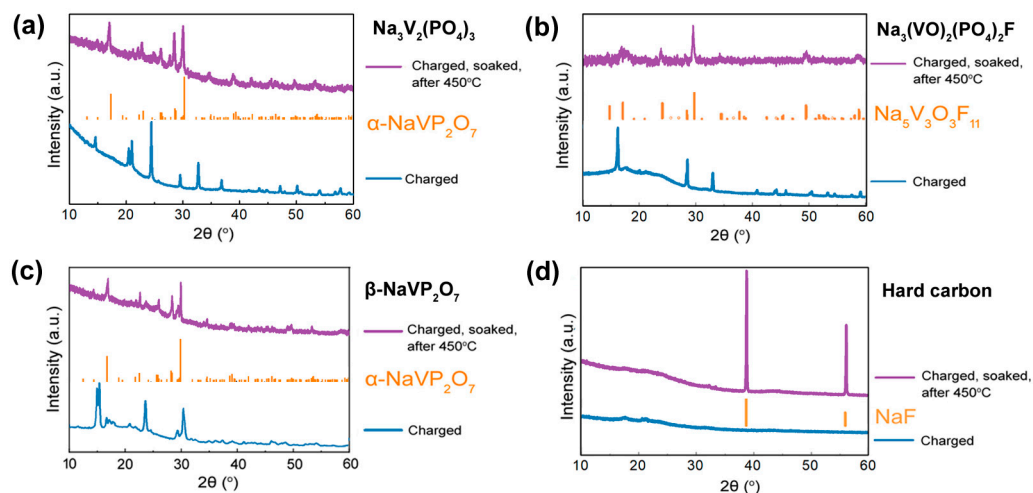
Figure 5. Results of ex situ PXRD for the charged electrodes soaked in 1M NaPF$_6$ in EC:DEC electrolyte before and after DSC experiments: Na$_3$V$_2$(PO$_4$)$_3$ (**a**), Na$_3$(VO)$_2$(PO$_4$)$_2$F (**b**), β–NaVP$_2$O$_7$ (**c**), and hard carbon (**d**).

According to the X-ray diffraction data (Figure 5), the decomposition products of NaV$_2$(PO$_4$)$_3$ and Na(VO)$_2$(PO$_4$)$_2$F in the presence of an electrolyte differ significantly from those of the dry electrodes described in literature [23]. This correlates well with the elevated values of thermal effects: while charged dry electrodes mainly produce desodiated phases after the DSC experiment, the presence of electrolytes results in the formation of sodium-containing pyrophosphate and oxofluoride (Figure 5, Table 2).

In the case of the anode material, the presence of electrolytes leads to similar results: the thermal effect of the decomposition increases while the onset and peak temperatures decrease (Figure 3, Table 2). The total enthalpy released during heating by the mixture of the charged hard carbon and electrolyte is 1205 J·g^{-1}. Hard carbon shows the highest increase in enthalpy compared to the "electrode+electrolyte" sum ($\approx$38%) among all the

studied samples (Figure 4). It is likely that the chemical interaction in the mixture during heating occurs in a manner similar to the formation of the solid–electrolyte interface (SEI). This process is well-known to proceed more intensely at the anode (i.e., reduction in the electrolyte) than at the cathode (oxidation of the electrolyte) side [37–40].

4. Discussion

The choice of a polyanionic cathode material for the development of sodium-ion battery technology is an extremely ambiguous task, since scientists and developers know a large family of different cathodes, each with its own advantages and disadvantages. In this paper, we studied such a key parameter of a sodium-ion battery as the thermal stability of the "electrode–electrolyte" combination for several vanadium-based cathode materials. Particularly, two of them are well-known and intensively studied—$Na_3V_2(PO_4)_3$ and $Na_3(VO)_2(PO_4)_2F$—and a third—β–$NaVP_2O_7$—was discovered much later than the others, but is gaining popularity, at least in laboratory studies. The inclusion of this material in this paper is also dictated by the fact that pyrophosphates are much more thermally stable than phosphates or fluoride phosphates, which means that the use of β–$NaVP_2O_7$ may be in demand in those areas where battery safety is more important than its weight and size characteristics [4]. Indeed, a comparison of the theoretical specific energy capacity of these cathodes does not speak in favor of $Na_3V_2(PO_4)_3$: ≈ 415 Wh kg^{-1} for $Na_3V_2(PO_4)_3$, ≈ 420 for β–$NaVP_2O_7$, and ≈ 480 for $Na_3(VO)_2(PO_4)_2F$. However, as the data presented in the article show, it exhibits less chemical activity during the thermal decomposition of the electrode wetted with an electrolyte: the increase in heat for β–$NaVP_2O_7$ (compared to the value for liquid electrolyte) was 36% versus 87% for $Na_3V_2(PO_4)_3$ and 71% for $Na_3(VO)_2(PO_4)_2F$.

For a deeper understanding of the results, it is necessary to compare the obtained data with the lithium-ion system, more precisely, with the most popular polyanionic material—$LiFePO_4$. There are some difficulties with this, since the literature data devoted to the study of the thermal stability of delithiated $LiFePO_4$ in "dry" form and in the presence of electrolytes are partly contradictory. Thus, Xiang et al., who studied the interaction of liquid electrolyte with various cathode materials, found that $LiFePO_4$ suppresses the decomposition of the electrolyte and reduces the magnitude of the thermal effect [24]. The authors explained this by the fact that some active groups on the surface (e.g., PO_4^{3-}) of the material interact with Lewis acid PF_5, which is a catalyst for the thermal decomposition of the electrolyte. On the other hand, Joachin et al., as well as Huang et al. and Yi et al., found a significant increase in the enthalpy of decomposition of $FePO_4$ in the presence of an electrolyte [3,5,41]. Joachin et al. estimated the thermal effect of the reaction at 145 J·g^{-1} (however, the authors did not indicate what exactly the thermal effect value was normalized to), Huang et al. at 251 J·g^{-1} (normalized to the mass of the electrode + the mass of the electrolyte, which was from 25 to 35% in the mixture), and Yi et al. 501 J·g^{-1} (normalized to the mass of the electrode material, with an electrode:electrolyte mass ratio = 1:2). Yamada et al. did not provide data for a "dry" electrode, but the one wetted with electrolytes showed thermal effect values similar to Joachin's—147 J·g^{-1} [42]. It is worth noting that, in this case, too, the authors did not indicate what exactly the thermal effect was normalized to. Thus, even among those researches who report an increase in the enthalpy of decomposition in contact with an electrolyte, there is no consensus on the values of thermal effects; this is probably largely due to different approaches to conducting the experiment. We performed our studies with hydrothermally synthesized $LiFePO_4$ and commercially available 1M $LiPF_6$ in EC:DEC:DMC = 1:1:1 (Figure 6a) and obtained a value of 276 J·g^{-1} (50 J·g^{-1} for an electrode without electrolyte), normalized to the mass of the electrode material (or 138 J·g^{-1}, if normalized to the sum of the masses of the electrode and electrolyte—i.e., using the approach of Huang et al.).
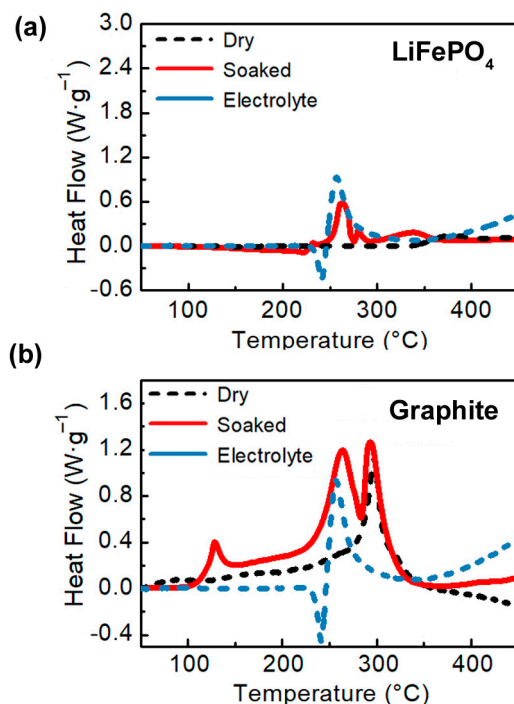
Figure 6. DSC curves (red line) for the charged Li-ion electrode materials soaked in electrolyte: LiFePO$_4$ (**a**) and graphite (**b**). For comparison, DSC curves for the dried electrodes (dot line) and 1M LiPF$_6$ in EC:DEC:DMC electrolyte (blue line) are also plotted.

The increase in heat release compared to a pure electrolyte in our experiment was 22%, which is less than for all studied sodium cathodes. Thus, even despite the better stability of the sodium-ion liquid electrolyte compared to the lithium-ion one, sodium-containing vanadium-based cathodes in a charged state demonstrate a greater increase in the enthalpy of decomposition in the presence of an electrolyte than LiFePO$_4$.

As for the anode material, the situation is rather the opposite. Wang et al. studied charged graphite in dry form and in the presence of an electrolyte and obtained the values of the thermal effect of decomposition of 1341 and 2253 J·g^{-1}, respectively (normalized to the mass of the electrode material; the mass ratio electrode:electrolyte = 1:1) [43]. In our experiment, under the same conditions, we obtained 449 and 2334 J·g^{-1} with the same normalization (Figure 6b). Thus, the thermal effect of the reaction of charged graphite with an electrolyte is higher than that of hard carbon (610 and 1205 J·g^{-1}, respectively).

5. Conclusions

To summarize the results, we would highlight the following observations.

Sodium-ion electrolytes, depending on their composition, begin to decompose when heated to 250~300 °C, which is 20–30 °C higher than the published temperatures for lithium electrolytes.

Vanadium-based polyanionic cathodes in contact with 1M NaPF$_6$ in the EC:DEC electrolyte demonstrate reduced decomposition temperatures and a more intense heat release in comparison with the dry state. The onset temperature depends on the desodiation potential; this effect may be a consequence of both a more reactive cathode–electrolyte interface and the previously described chemical interaction of vanadium cations with electrolyte components. However, in terms of decomposition enthalpy, β-NaVP$_2$O$_7$ demonstrates a better behavior compared to Na$_3$V$_2$(PO$_4$)$_3$ and Na$_3$(VO)$_2$(PO$_4$)$_2$F despite its high charging potential.

The least stable part of the sodium-ion electrochemical cell is the anode material. In the presence of electrolytes, it demonstrates almost a 40% increase in decomposition enthalpy and a shift of the main peak maxima from 273 to 238 °C. However, both the increase in the

heat of the decomposition of hard carbon in the presence of electrolytes and its absolute value are less than similar parameters for graphite in a lithium-ion system, in accordance with the literature data and the results of our own experiments.

Overall, the significant increase in the thermal effect of the decomposition of "charged material–electrolyte" mixtures compared to "dry" electrodes confirms the widespread belief that the liquid electrolyte is the main source of safety problems in metal-ion batteries. To eliminate these shortcomings, it is necessary to develop solid-state secondary current sources using polymeric and/or ceramic electrolyte materials.

References

1. Liu, B.; Jia, Y.; Yuan, C.; Wang, L.; Gao, X.; Yin, S.; Xu, J. Safety Issues and Mechanisms of Lithium-Ion Battery Cell upon Mechanical Abusive Loading: A Review. *Energy Storage Mater.* **2020**, *24*, 85–112. [CrossRef]
2. Martha, S.K.; Haik, O.; Zinigrad, E.; Exnar, I.; Drezen, T.; Miners, J.H.; Aurbach, D. On the Thermal Stability of Olivine Cathode Materials for Lithium-Ion Batteries. *J. Electrochem. Soc.* **2011**, *158*, A1115. [CrossRef]
3. Huang, Y.; Lin, Y.C.; Jenkins, D.M.; Chernova, N.A.; Chung, Y.; Radhakrishnan, B.; Chu, I.H.; Fang, J.; Wang, Q.; Omenya, F.; et al. Thermal Stability and Reactivity of Cathode Materials for Li-Ion Batteries. *ACS Appl. Mater. Interfaces* **2016**, *8*, 7013–7021. [CrossRef]
4. Tamaru, M.; Chung, S.C.; Shimizu, D.; Nishimura, S.I.; Yamada, A. Pyrophosphate Chemistry toward Safe Rechargeable Batteries. *Chem. Mater.* **2013**, *25*, 2538–2543. [CrossRef]
5. Yi, J.; Wang, C.; Xia, Y. Comparison of Thermal Stability between Micro- and Nano-Sized Materials for Lithium-Ion Batteries. *Electrochem. Commun.* **2013**, *33*, 115–118. [CrossRef]
6. Lee, Y.; Kim, S.O.; Mun, J.; Park, M.S.; Kim, K.J.; Lee, K.Y.; Choi, W. Influence of Salt, Solvents, and Additives on the Thermal Stability of Delithiated Cathodes in Lithium-Ion Batteries. *J. Electroanal. Chem.* **2017**, *807*, 174–180. [CrossRef]
7. Gnanaraj, J.S.; Zinigrad, E.; Asraf, L.; Gottlieb, H.E.; Sprecher, M.; Schmidt, M.; Geissler, W.; Aurbach, D. A Detailed Investigation of the Thermal Reactions of LiPF6 Solution in Organic Carbonates Using ARC and DSC. *J. Electrochem. Soc.* **2003**, *150*, A1533. [CrossRef]
8. Golubkov, A.W.; Fuchs, D.; Wagner, J.; Wiltsche, H.; Stangl, C.; Fauler, G.; Voitice, G.; Thalera, A.; Hacker, V. Thermal-runaway experiments on consumer Li-ion batteries with metal-oxide and olivin-type cathodes. *RSC Adv.* **2014**, *4*, 3633–3642. [CrossRef]
9. Velumani, D.; Bansal, A. Thermal Behavior of Lithium- and Sodium-Ion Batteries: A Review on Heat Generation, Battery Degradation, Thermal Runway—Perspective and Future Directions. *Energy Fuels* **2022**, *36*, 14000–14029. [CrossRef]
10. Bang, H.; Kim, D.-H.; Bae, Y.C.; Prakash, J.; Sun, Y.-K. Effects of Metal Ions on the Structural and Thermal Stabilities of $Li[Ni_{1-x-y}Co_xMn_y]O_2$ ($x + y \leq 0.5$) Studied by In Situ High Temperature XRD. *J. Electrochem. Soc.* **2008**, *155*, A952–A958. [CrossRef]
11. Sun, Y.K.; Myung, S.T.; Park, B.C.; Prakash, J.; Belharouak, I.; Amine, K. High-energy cathode material for long-life and safe lithium batteries. *Nat. Mater.* **2009**, *8*, 320–324. [CrossRef] [PubMed]
12. Bak, S.-M.; Hu, E.; Zhou, Y.; Yu, X.; Senanayake, S.D.; Cho, S.-J.; Kim, K.-B.; Chung, K.Y.; Yang, X.-Q.; Nam, K.-W. Structural Changes and Thermal Stability of Charged $LiNi_xMn_yCo_zO_2$ Cathode Materials Studied by Combined In Situ Time-Resolved XRD and Mass Spectroscopy. *ACS Appl. Mater. Interfaces* **2014**, *6*, 22594–22601. [CrossRef] [PubMed]
13. Song, Y.; Cui, Y.; Li, B.; Geng, L.; Yan, J.; Zhu, D.; Zhou, P.; Zhou, J.; Yan, Z.; Xue, Q.; et al. Revealing the origin of high-thermal-stability of single-crystal Ni-rich cathodes toward higher-safety batteries. *Nano Energy* **2023**, *116*, 108846. [CrossRef]
14. Zhao, J.; Xu, J.; Lee, D.H.; Dimov, N.; Meng, Y.S.; Okada, S. Electrochemical and Thermal Properties of P2-Type $Na_{2/3}Fe_{1/3}Mn_{2/3}O_2$ for Na-Ion Batteries. *J. Power Sources* **2014**, *264*, 235–239. [CrossRef]

15. Zuo, W.; Liu, R.; Ortiz, G.F.; Rubio, S.; Chyrka, T.; Lavela, P.; Zheng, S.; Tirado, J.L.; Wang, D.; Yang, Y. Sodium Storage Behavior of $Na_{0.66}Ni_{0.33}$-xZnxMn$_{0.67}O_2$ (x = 0, 0.07 and 0.14) Positive Materials in Diglyme-Based Electrolytes. *J. Power Sources* **2018**, *400*, 317–324. [CrossRef]

16. Zhao, J.; Zhao, L.; Chihara, K.; Okada, S.; Yamaki, J.I.; Matsumoto, S.; Kuze, S.; Nakane, K. Electrochemical and Thermal Properties of Hard Carbon-Type Anodes for Na-Ion Batteries. *J. Power Sources* **2013**, *244*, 752–757. [CrossRef]

17. Ponrouch, A.; Marchante, E.; Courty, M.; Tarascon, J.M.; Palacín, M.R. In Search of an Optimized Electrolyte for Na-Ion Batteries. *Energy Environ. Sci.* **2012**, *5*, 8572–8583. [CrossRef]

18. Li, Z.; Dadsetan, M.; Gao, J.; Zhang, S.; Cai, L.; Naseri, A.; Jimenez-Castaneda, M.E.; Filley, T.; Miller, J.T.; Thomson, M.J.; et al. Revealing the Thermal Safety of Prussian Blue Cathode for Safer Nonaqueous Batteries. *Adv. Energy Mater.* **2021**, *11*, 2101764. [CrossRef]

19. Ge, L.; Song, Y.; Niu, P.; Li, B.; Zhou, L.; Feng, W.; Ma, C.; Li, X.; Kong, D.; Yan, Z.; et al. Elaborating the Crystal Water of Prussian Blue for Outstanding Performance of Sodium Ion Batteries. *ACS Nano* **2024**, *18*, 3542–3552. [CrossRef]

20. Zhang, X.; Dong, X.; Qiu, X.; Cao, Y.; Wang, C.; Wang, Y.; Xia, Y. Extended low-voltage plateau capacity of hard carbon spheres anode for sodium ion batteries, Extended low-voltage plateau capacity of hard carbon spheres anode for sodium ion batteries. *J. Power Sources* **2020**, *476*, 228550. [CrossRef]

21. Mohsin, I.U.; Hofmann, A.; Ziebert, C. Exploring the reactivity of $Na_3V_2(PO_4)_3$/C and hard carbon electrodes in sodium-ion batteries at various charge states. *Electrochim. Acta* **2024**, *487*, 144197. [CrossRef]

22. Samigullin, R.R.; Zakharkin, M.V.; Drozhzhin, O.A.; Antipov, E.V. Thermal Stability of NASICON-Type $Na_3V_2(PO_4)_3$ and $Na_4VMn(PO_4)_3$ as Cathode Materials for Sodium-ion Batteries. *Energies* **2023**, *16*, 3051. [CrossRef]

23. Samigullin, R.R.; Drozhzhin, O.A.; Antipov, E.V. Comparative Study of the Thermal Stability of Electrode Materials for Li-Ion and Na-Ion Batteries. *ACS Appl. Energy Mater.* **2022**, *5*, 14–19. [CrossRef]

24. Xiang, H.F.; Wang, H.; Chen, C.H.; Ge, X.W.; Guo, S.; Sun, J.H.; Hu, W.Q. Thermal stability of LiPF6-based electrolyte and effect of contact with various delithiated cathodes of Li-ion batteries. *J. Power Sources* **2009**, *191*, 575–581. [CrossRef]

25. Chen, G.; Richardson, T.J. Thermal instability of Olivine-type LiMnPO4 cathodes. *J. Power Sources* **2010**, *195*, 1221–1224. [CrossRef]

26. He, X.; Ping, P.; Kong, D.; Wang, G.; Wang, D. Comparison study of electrochemical and thermal stability of $Na_3V_2(PO_4)_3$ in different electrolytes under room and elevated temperature. *Int. J. Energy Res.* **2022**, *46*, 23173–23194. [CrossRef]

27. Eshetu, G.G.; Grugeon, S.; Kim, H.; Jeong, S.; Wu, L.; Gachot, G.; Laruelle, S.; Armand, M.; Passerini, S. Comprehensive Insights into the Reactivity of Electrolytes Based on Sodium Ions. *ChemSusChem* **2016**, *9*, 462. [CrossRef]

28. Gan, Y.; Ping, P.; Wang, J.; Song, Y.; Gao, W. Comparative analysis of thermal stability and electrochemical performance of NaNi$_{1/3}$Fe$_{1/3}$Mn$_{1/3}$O$_2$ cathode in different electrolytes for sodium ion batteries. *J. Power Sources* **2024**, *594*, 234008. [CrossRef]

29. Zakharkin, M.V.; Drozhzhin, O.A.; Ryazantsev, S.V.; Chernyshov, D.; Kirsanova, M.A.; Mikheev, I.V.; Pazhetnov, E.M.; Antipov, E.V.; Stevenson, K.J. Electrochemical properties and evolution of the phase transformation behavior in the NASICON-type $Na_{3+x}Mn_xV_2$-x(PO$_4$)$_3$ (0 ≤ x ≤ 1) cathodes for Na-ion batteries. *J. Power Sources* **2020**, *470*, 228231. [CrossRef]

30. Burova, D.; Shakhova, I.; Morozova, P.; Iarchuk, A.; Drozhzhin, O.A.; Rozova, M.G.; Praneetha, S.; Murugan, V.; Tarascon, J.M.; Abakumov, A.M. The Rapid Microwave-Assisted Hydrothermal Synthesis of NASICON-Structured $Na_3V_2O_2$: X(PO$_4$)$_2$F$_3$-$_2$ x (0 < x ≤ 1) Cathode Materials for Na-Ion Batteries. *RSC Adv.* **2019**, *9*, 19429–19440. [CrossRef]

31. Drozhzhin, O.A.; Tertov, I.V.; Alekseeva, A.M.; Aksyonov, D.A.; Stevenson, K.J.; Abakumov, A.M.; Antipov, E.V. β-NaVP2O7 as a Superior Electrode Material for Na-Ion Batteries. *Chem. Mater.* **2019**, *31*, 7463–7469. [CrossRef]

32. Bobyleva, Z.V.; Drozhzhin, O.A.; Alekseeva, A.M.; Dosaev, K.A.; Peters, G.S.; Lakienko, G.P.; Perfilyeva, T.I.; Sobolev, N.A.; Maslakov, K.I.; Savilov, S.V.; et al. Caramelization as a Key Stage for the Preparation of Monolithic Hard Carbon with Advanced Performance in Sodium-Ion Batteries. *ACS Appl. Energy Mater.* **2023**, *6*, 181–190. [CrossRef]

33. Wang, J.; Yamada, Y.; Sodeyama, K.; Chiang, C.H.; Tateyama, Y. Superconcentrated electrolytes for a high-voltage lithium-ion battery. *Nat. Commun.* **2016**, *7*, 12032. [CrossRef] [PubMed]

34. Hou, J.; Lu, L.; Wang, L.; Ohma, A.; Ren, D.; Feng, X.; Li, Y.; Li, Y.; Ootani, I.; Han, X.; et al. Thermal runaway of Lithium-ion batteries employing LiN(SO$_2$F)$_2$-based concentrated electrolytes. *Nat. Commun.* **2020**, *11*, 5100. [CrossRef] [PubMed]

35. Zhao, L.; Inoishi, A.; Okada, S. Thermal risk evaluation of concentrated electrolytes for Li-ion batteries. *J. Power Sources Adv.* **2021**, *12*, 100079. [CrossRef]

36. Pablos, C.; Olchowka, J.; Petit, E.; Minart, G.; Duttine, M.; Weill, F.; Masquelier, C.; Carlier, D.; Croguennec, L. Thermal Stability of Na_3–xV$_2$(PO$_4$)$_2$F$_3$–yOy: Influence of F– for O$_2$– Substitution and Degradation Mechanisms. *Chem. Mater.* **2023**, *35*, 4078–4088. [CrossRef]

37. Gauthier, M.; Carney, T.J.; Grimaud, A.; Giordano, L.; Pour, N.; Chang, H.-H.; Fenning, D.P.; Lux, S.F.; Paschos, O.; Bauer, C.; et al. Electrode–Electrolyte Interface in Li-Ion Batteries: Current Understanding and New Insights. *J. Phys. Chem. Lett.* **2015**, *6*, 4653–4672. [CrossRef] [PubMed]

38. Meng, J.; Jia, G.; Yang, H.; Wang, M. Recent advances for SEI of hard carbon anode in sodium-ion batteries: A mini review. *Front. Chem.* **2022**, *10*, 986541. [CrossRef] [PubMed]

39. Daboss, S.; Philipp, T.; Palanisamy, K.; Flowers, J.; Stein, H.S.; Kranz, C. Characterization of the solid/electrolyte interphase at hard carbon anodes via scanning (electrochemical) probe microscopy. *Electrochim. Acta* **2023**, *453*, 142345. [CrossRef]

40. Pan, Y.; Zhang, Y.; Parimalam, B.S.; Nguyen, C.C.; Wang, G.; Lucht, B.L. Investigation of the solid electrolyte interphase on hard carbon electrode for sodium ion batteries. *J. Electroanal. Chem.* **2017**, *799*, 181–186. [CrossRef]

41. Joachin, H.; Kaun, T.D.; Zaghib, K.; Prakash, J. Electrochemical and Thermal Studies of Carbon-Coated LiFePO$_4$ Cathode. *J. Electrochem. Soc.* **2009**, *156*, A401–A406. [CrossRef]

42. Yamada, A.; Chung, S.C.; Hinokuma, K. Optimized LiFePO$_4$ for Lithium Battery Cathodes. *J. Electrochem. Soc.* **2001**, *148*, A224–A229. [CrossRef]

43. Wang, Q.; Sun, J.; Yao, X.; Chen, C. Thermal Behavior of Lithiated Graphite with Electrolyte in Lithium-Ion Batteries. *J. Electrochem. Soc.* **2006**, *153*, A329–A333. [CrossRef]